Research Article Vol. 30, No. 4 / 14 Feb 2022 / Optics Express 6332
Optics EXPRESS

Fiber pigtailed DFB laser-based optical feedback cavity enhanced absorption spectroscopy with a fiber-coupled EOM for phase correction

XIAOBIN ZHOU,[1,2] GANG ZHAO,[1,2,3] JIANXIN LIU,[1,2] YUETING ZHOU,[1,2] XIAOJUAN YAN,[1,2] ZHIXIN LI,[1,2] WEIGUANG MA,[1,2,4] AND SUOTANG JIA[1,2]

[1] *State Key Laboratory of Quantum Optics and Quantum Optics Devices, Institute of Laser Spectroscopy, Shanxi University, Taiyuan 030006, China*
[2] *Collaborative Innovation Center of Extreme Optics, Shanxi University, Taiyuan 030006, China*
[3] *gangzhao@sxu.edu.cn*
[4] *mwg@sxu.edu.cn*

Abstract: A novel technique for performing fiber pigtailed DFB laser and linear Fabry-Pérot cavity based optical feedback cavity enhanced absorption spectroscopy (OF-CEAS) is proposed. A fiber-coupled electro-optic modulator (f-EOM) with x-cut y-propagation $LiNbO_3$ waveguide is employed, instead of PZT used in traditional OF-CEAS, to correct the feedback phase, which improves the compactness and applicability of OF-CEAS. Through the efficient and real-time control of the feedback phase by actively changing the input voltage of the f-EOM, a good long-term stability of the signal has been achieved. Consequently, a detection sensitivity down to 7.8×10^{-10} cm^{-1}, better than the previous by PZT based OF-CEAS, has been achieved over the integration time of 200 s, even by use of a cavity with moderate finesse of 2850.

© 2022 Optica Publishing Group under the terms of the Optica Open Access Publishing Agreement

1. Introduction

Laser absorption spectroscopy (LAS) is a new type of technique for trace gas detection, which has the merits of real-time, high sensitivity, and free of pre-sampling. Tunable diode laser absorption spectroscopy (TDLAS) [1,2], the most basic and popular LAS, could result in a detection sensitivity, in terms of absorption coefficient, down to 10^{-5}. It has been applied in different fields, including industrial process control, air quality monitoring, hazardous gas detection and so on. However, its performance is insufficient to be utilized in the scenario that demands higher sensitivity.

Cavity-based LAS is a good alternative, which uses an optical cavity, composed of high-reflectivity mirrors, to greatly improve the interaction length between the laser and the target gas. As a result, the detection sensitivity is enhanced. The enhancement factor can be expressed as $2F/\pi$, where F is the cavity finesse, roughly equal to $\pi/(1-R)$ with R defined as the power reflectivity of the cavity mirror [3]. Benefiting from superb coating technique, the mirror with R higher than 99.999% can be made in near infrared (NIR) wavelength range [4], therefore a cavity with enhancement factor larger than 3×10^5 can be reasonably manufactured. This implies that the interaction length could be longer than 10 km and the sensitivity could reach to 10^{-10} level. Direct measurement of the amplitude attenuation of the cavity transmission modes, so called cavity enhanced direct absorption spectroscopy (CEAS), is a basic cavity-based technique. However, its sensitivity is difficult to get to 10^{-10} level due to the unstable and weak amplitudes of the cavity modes, caused by the discrepancy between the laser frequency and the cavity longitudinal mode. This phenomenon becomes more serious especially for diode lasers which are the most common light sources in trace gas detection fields but possess linewidth in the MHz range. To solve this, commonly, two strategies can be used. The first is to perform

#449938 https://doi.org/10.1364/OE.449938
Journal © 2022 Received 29 Nov 2021; revised 2 Feb 2022; accepted 4 Feb 2022; published 11 Feb 2022

Optics EXPRESS

cavity ringdown spectroscopy (CRDS) [5,6], which can deduce the intracavity absorption by the difference between the ringdown times with and without sample inside the cavity, rather than the amplitude attenuation of the cavity modes. Hence it is immune to laser power noise. Nevertheless, the faint cavity transmission caused by the low coupling efficiency will deteriorate signal-to-noise ratio of the ringdown signal and thus the performance for trace gas detection.

The alternative method is to perform optical feedback CEAS (OF-CEAS). In this process, the frequency noise of the laser can be squeezed into the bandwidth of cavity mode by optical feedback which is usually thought harmful to an application of diode laser. As a consequence, the coupling efficiency is greatly improved. Moreover, because of the purification of laser relative intensity noise by optical feedback [7], the performance for trace gas detection has potential to be the same with, or even better than, that of CRDS.

In 2005, OF-CEAS was first proposed by J. Morville et. al. based on a V-shape cavity. This cavity geometry can avoid the direction reflection from the cavity front mirror into the laser [8,9]. Afterwards, series works based on a linear Fabry-Pérot (FP) cavity have been reported, in which extra measures to suppress the direct reflection, such as mode mismatch between laser and cavity [10,11], feedback using the transmitted light [12], are utilized. Recently, we have theoretically and experimentally demonstrated that OF-CEAS cooperated with a linear cavity could be realized using a simple scheme since the direct reflection does not generate effective optical feedback at cavity longitudinal modes if the optical feedback phase is properly controlled. And this novel scheme dramatically improves the universality and applicability of OF-CEAS [13]. Up to now, most OF-CEAS experiments were based on a diode laser with free space output because it is convenient to estimate and control the feedback phase and the feedback ratio. In 2019, a fiber pigtailed diode laser was used to perform the optical feedback CRDS, which can make the feedback optical path more compact especially for a long cavity [14].

In OF-CEAS, to stimulate desired feedback, the feedback phase at the cavity mode frequencies should be a multiple of 2π. This is roughly realized by adjusting the distance, between the laser and the cavity front mirror, to approximately equal an integer multiple of the cavity length. As a result, a long spatial light path is necessary and makes the spectrometer more sensitive to the mechanical vibration. In addition, in order to get a long-term stable system, the delicate and real-time control of the feedback phase is indispensable. Traditionally, this is accomplished by a piezo-transducer (PZT) attached to a reflector placed in the light path [11,15]. By detuning the PZT's driving voltage to stretch the PZT length, the light path length as well as the feedback phase is regulated. PZT is made of ceramics and its displacement depends both on the strain and the electrical field. This makes it sensitive to mechanical vibration and acoustic noise [16]. And the bandwidth of PZT is relatively slow, normally in tens of kHz range, thereby is difficult to compensate the phase noises in high frequency region. Moreover, if the stretching direction of the PZT is not parallel to the light route, the optical alignment will vary slightly, which results in a deteriorated CEAS signal to some extent.

In this paper, a FP cavity and a fiber pigtailed DFB laser are used together to perform OF-CEAS. To avoid the problem given by the PZT, a fiber-coupled electro-optic phase modulator (f-EOM) is utilized to control the feedback phase by regulating its input voltage. Special care has been taken to avoid the stimulation of optical feedback by the surfaces of the fiber components. Then, C_2H_2 is chosen as the target gas to evaluate the performance of this OF-CEAS system. The experimental details are presented and finally the stability, sensitivity and linearity are tested.

2. Experimental setup

The diagram of the experimental setup is shown in Fig. 1. The light source is a polarization maintaining (PM) fiber pigtailed DFB laser, emitted at 1.53 μm with output power of 10 mW. The laser frequency is scanned by varying its injection current with a triangular wave signal. After passing through a f-EOM (Photline, MPX-LN-0.5) with x-cut y-propagation LiNbO3 waveguide

Optics EXPRESS

fabricated by titanium diffusion, the laser is sent into free space by a fiber collimator. The spatial light propagates through, in sequence, a mode match lens, a half-wave plate (λ/2), a polarizing beam splitter (PBS) and a quarter-wave plate (λ/4). The mode-matched power coupling fraction of 50% has been resulted. The λ/2 is used to maximize the transmission of the PBS. And the combination of the PBS and the λ/4 is for the adjustment of the feedback ratio. The optical components are slightly tilted so as to reduce unfavorable laser interference. On the other hand, a small part of light is separated by a beam splitter (BS) with ratio of 1:9, directed to a photodetector (PD_1) and worked as a non-absorption laser power reference.

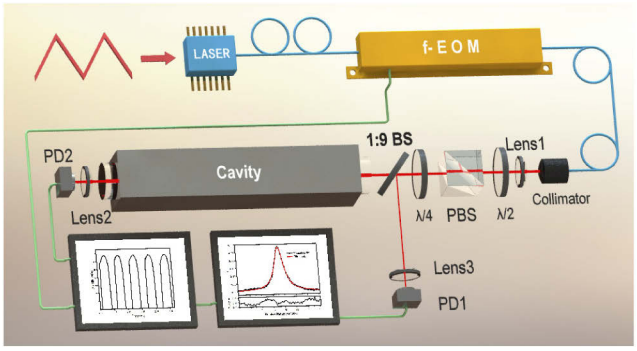

Fig. 1. Schematic diagram of the experimental setup. f-EOM, fiber-coupled electro-optic modulator; PBS, polarizing beam splitter; λ/2, half-wave plate; λ/4, quarter-wave plate; BS, beam splitter; PD, photodetector.

While, most of the light is impinged onto a FP cavity. The cavity is composed of two mirrors with reflectivity of 99.89%, confirmed by an additional cavity ringdown spectroscopy experiment and corresponding to the cavity finesse of around 2850. The two cavity mirrors are spaced by a invar tube with low thermal expansion coefficient, by a distance of 39 cm, indicating a free spectral region (FSR) of 375 MHz. The intracavity light leakage, incorporated with the direct reflection from the cavity front mirror, is returned back to the diode laser to generate optical feedback. As demonstrated by our previous work, if the feedback phase is properly controlled, the frequency locking of the laser to the cavity mode could be achieved which results in high coupling efficiency [17]. The cavity transmission is detected by a photodetector (PD_2) and then recorded by a data acquisition card. To carry out CEAS, the amplitude of each cavity mode, which is relative to the intracavity absorption, is extracted.

Comparisons between the PZT [13] and the f-EOM based OF-CEAS have been made, which shows that acoustic noise could introduce noise into the PZT based system, while no influence has been observed in the other. And 10 μm stretching of the PZT could lead to the variation of the beam position in the order of μm measured with a beam profiler located 2 m away from the PZT.

3. Control of the feedback ratio and the feedback phase

In the process of optical feedback, two parameters, i.e., feedback ratio and feedback phase, are crucial and required to be controlled deliberately [18]. The feedback ratio should be confined in a region around 10^{-4}, where a desired optical feedback regime can be resulted [19]. In order to realize this situation, in our setup, the λ/4 is finely rotated to adjust the ratio of the returned light passing through the PBS without loss of power to the cavity. However, besides this, the unwanted optical feedback by the reflection from the surface of other optical components, especially the surfaces of the EOM crystal and the interface of the fiber, had been observed, leading to a feedback competition with the cavity leakage. To solve this problem, an isolator with rejection ratio of 25 dB is integrated inside the DFB laser and the output fiber of the laser is welded

Optics EXPRESS

together with the input fiber of the f-EOM. The welding also brings an extra merit that the power loss from the fiber adapter is avoided and thus higher transmission power is obtained. In addition, the optical components are anti-reflection coated in their surfaces. By these efforts, the long-term stability of optical feedback exclusively stimulated by the FP cavity is resulted.

To make sure that the feedback phase at each cavity mode equals a multiple of 2π, the optical path between the laser and the cavity front mirror should be controlled to equal a multiple of the cavity length. In the first step, the collimator is mounted on a translation stage to coarsely adjust the distance. Then, a fine and real-time phase compensation is realized by controlling the input voltage of the f-EOM by an electric feedback servo to adjust the light phase. The phase modulation bandwidth for the f-EOM is from DC to 500 MHz. Due to the fact that the half wave voltage of the f-EOM, i.e., V_π, is around 4 V, the phase tuning range of 5π could be obtained with a full input voltage range of 20 V. This corresponds to an optical path adjustable range of around 3.75 μm for laser at a wavelength of 1.5 μm. This is much larger than the optical path variation, which is measured to be less than 1.5 μm within half an hour, induced by external disturbance in our system. The error signal for the real-time phase control is generated by judging the asymmetry of the cavity mode, which is based on the subtraction of the areas of the two regions segmented by the center line of each cavity mode. The judgement process is implemented by a LabVIEW program. Subsequently, a correction signal is output and then sent to the DC port of the f-EOM. Figure 2 illustrates the measured cavity transmission modes under different DC offset voltages to the f-EOM when the laser frequency is scanned. The Fig. 2(a) shows the results when the offset voltage deviates from the desired operating point, that presents a right asymmetry. An even larger phase deviation would give rise to the attenuation of the cavity modes and hence introduce error into the CEAS [8]. The Fig. 2(b) shows the modes when the DC offset has a deviation in the opposite direction, which causes a left asymmetry. By feeding back the correction signal to the f-EOM, the optical feedback phase is regulated to satisfy the demand of the optimum optical feedback condition. Consequently, the cavity modes with symmetric profile are obtained, depicted in Fig. 2(c), even with large laser frequency scanning range. While, for an optical phase sensitive experiment, the direct employment of fiber components without special cares will definitely deteriorate the results due to the temperature or fiber bending caused drifts of optical path in fibers. To relieve this, in this experiment, the f-EOM and most of the fiber are housed in a temperature controlled copper block with temperature stability better than 0.001 °C. By estimation, the effective optical path between the laser and the cavity is around 156 cm, close

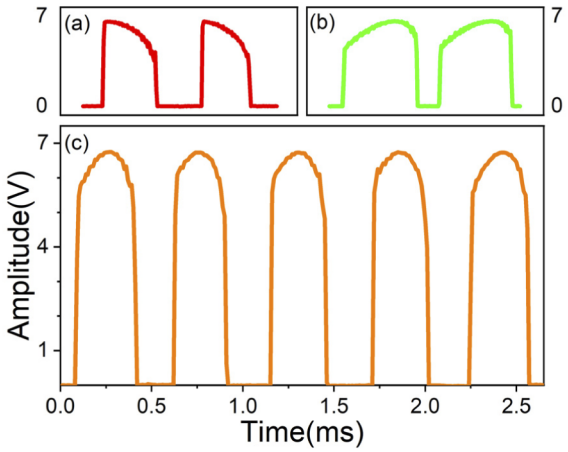

Fig. 2. The cavity transmission modes under different DC bias of the EOM

Optics EXPRESS

to the four times of cavity length, while the spatial light path for mode matching and convenient optical alignment is about 20 cm, which is shorter than the length requirement of total spatial coupled OF-CEAS. Thus, a more compact design is obtained

4. Experimental results

To verify the ability of the OF-CEAS system for trace gas detection, acetylene (C_2H_2) is used as the target gas. The high sensitive detection of C_2H_2 concentration in real time is highly significant in many fields, such as ethylene production process [20], leak detection during calcium carbide storage and transportation, understanding of chemiluminescence reaction, improvement of combustion efficiency [21], and analysis of soot generation [22]. In addition, in pathological diagnosis, measurement of C_2H_2, as a foreign gas or biomarker, could be used for non-invasive monitoring of heart function [23] and the effect of smoking on human metabolism [24,25].

In this experiment, an acetylene transition at 6529.17 cm^{-1} with linestrength of 1.165×10^{-20} cm^{-1}/(molecule·cm^{-2}) is aimed. In the measurement process, the cavity is filled with 1.5 ppm C_2H_2 at 0.92 atm (the local atmospheric pressure). To obtain a complete absorption spectrum, the laser frequency is continually detuned with a range of 23 GHz and 61 cavity modes are observed, shown as a black curve in Fig. 3. As can be seen, each mode owns high signal-to-noise ratio as the curve in Fig. 2(c). The attenuation of the amplitude of the cavity modes, caused by the intracavity absorption, could be clearly seen in the middle region. And there is also a linear variation in the background amplitudes of the cavity modes, attributed to the intrinsic change of the laser intensity originating from its driving current. This background variation along with laser relative intensity noise, namely non-absorption laser intensity, is eliminated by the balanced detection [26]. And the common-mode rejection ratio by the balanced detection is estimated to be 6.

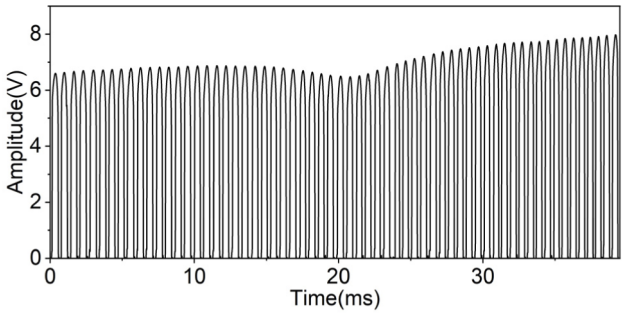

Fig. 3. The consecutive cavity transmission modes with absorption from acetylene.

With the above-mentioned measures, stable and sophisticated OF-CEAS signals are resulted and high sensitivity for trace gas detection is promising. In the signal processing, the maximum amplitudes of the cavity modes are extracted by the LabVIEW program, and the amplitude attenuation rates, i.e., $\Delta I(\nu)/I_0(\nu)$, are shown as black dots in Fig. 4(a). The x axis corresponds to the relative optical frequency which is calibrated by the cavity FSR. The attenuation rates as functions of the cavity parameters and the gas absorption can be expressed as [13]:

$$\frac{\Delta I(\nu)}{I_0(\nu)} = \frac{I_0(\nu) - I_t(\nu)}{I_0(\nu)} = 1 - \frac{(1-r^2)^2 \exp[-2\alpha(\nu)L]}{\{1 - r^2 exp[-2\alpha(\nu)L]\}^2} \tag{1}$$

where I_0 and I_t are the laser intensities without and with absorption, respectively; ΔI represents the intensity attenuation; ν is the laser frequency, r is the electric-field reflectivity of the cavity mirror, L is the cavity length and $\alpha(\nu)$ is the gas absorption coefficient.

Optics EXPRESS

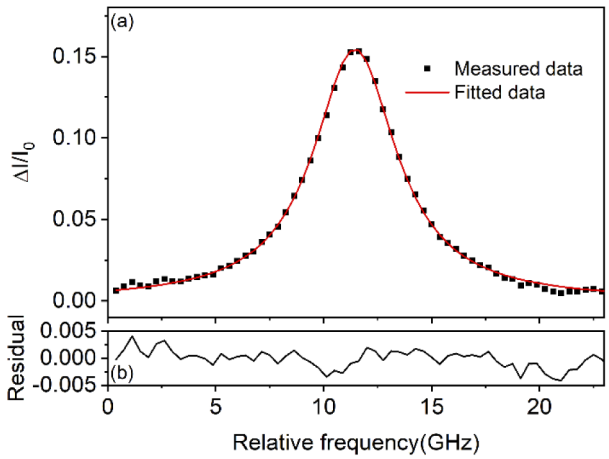

Fig. 4. (a) The retrieved intensity attenuation ratio by C_2H_2 absorption (black dots), and the Lorentzian fitting result (red line); (b) The fitting residuals.

The red line in Fig. 4(a) is the fitting result by the model in Eq. (1). In the simulation of the absorption lineshape, a Lorentzian function is used since the pressure broadening dominates the spectral linewidth. The adopted spectral parameters, including linestrength, air-broadened half width and self-broadened half width, are from the HITRAN2016 database [27]. The lower panel shows the fitting residual. Good consistency between the measurement and the model and the signal to noise ratio (SNR) of 114 has been achieved. The main limitation to the SNR is spurious interference, i.e., etalon effect, which is responsible for the structure in the residual.

In order to evaluate the long-term stability and the detection sensitivity of the system, a series of absorption signals for a certain concentration of C_2H_2 gas are measured at a rate of 0.5 Hz for more than 4 hours. The retrieved concentrations, displayed as black dots in Fig. 5(a), are around 1.52 ppm. The black line in the lower panel is the corresponding Allan-Werle plot [28]. For the integration time shorter than 50 s, the system shows a white noise response with a slope of 8.7×10^{-9} $cm^{-1} \cdot Hz^{-1/2}$, illustrated by the dash line in red. And it reaches to the minimum at 200 s, indicating a detection sensitivity of 7.8×10^{-10} cm^{-1} and a minimal detectable C_2H_2 concentration of 0.7 ppb. The detection sensitivity is 1.7 times better than the previous result by PZT based OF-CEAS [13], even though the cavity finesse in this work is 27% lower. Furthermore, these results are comparable to that by CRDS, which demonstrates the combination of optical feedback and balanced detection could suppress most of laser power noise caused by the laser relative intensity noise and laser to cavity coupling noise. With increasing integration times, the Allan deviation increases, possibly due to the drift of the etalon effect. A better long-term performance could be improved by the suppression of spurious interference.

Finally, to verify the linear response of the system, samples with a variety of C_2H_2 concentrations from 100 ppb to 9 ppm, obtained by mixing a standard C_2H_2 gas and a pure nitrogen with different ratios, were assessed. A successive measurement over 3 min has been executed for each gas sample. The average of the retrieved concentrations are shown as black triangle dots in Fig. 6. The red line is the linear fitting result with a slope of 1.001, an intercept of 1.03×10^{-9} and a R-square of 0.99989, which indicates a good linear dependence of the system on the gas concentration.

Optics EXPRESS

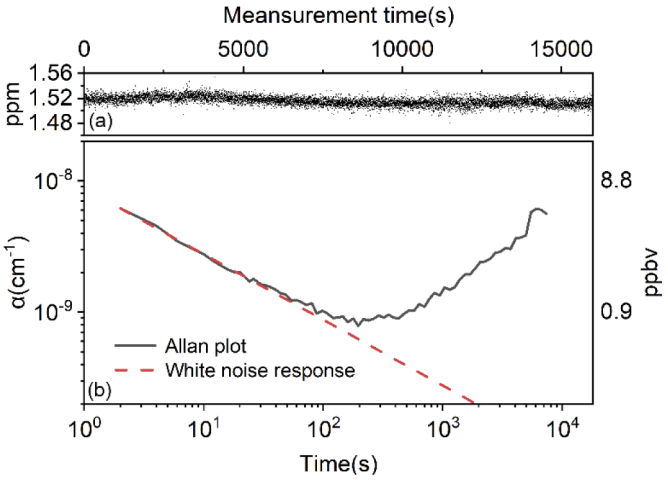

Fig. 5. (a) The retrieved concentrations from a long-term measurement of one set of C_2H_2 gas; (b) the Allan-Werle plot (black curve) and the white noise response (dash line in red).

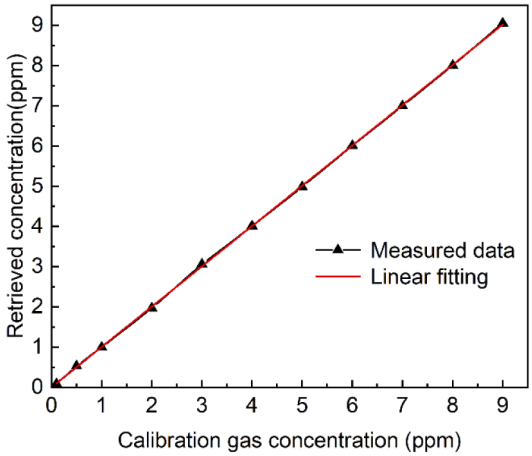

Fig. 6. The response of the system to different C_2H_2 concentration from 100 ppb to 9 ppm (triangle in black) and the linear fitting result (red line).

5. Conclusion

A fiber pigtailed DFB laser and linear FP cavity based OF-CEAS is performed. A fiber-coupled EOM with x-cut y-propagation $LiNbO_3$ waveguide, instead of the PZT used in traditional OF-CEAS setup, is used to regulate the optical feedback phase, which improves the dynamic laser alignment. The spatial light path is set to 20 cm for mode matching and convenient optical alignment, which is shorter than the length requirement of total spatial OF-CEAS. Thus a more compact system is resulted and better mechanical stability could be expected. In order to eliminate the influence of laser power fluctuation on the absorption signal, a balanced detection method is adopted. Then a series of absorption signals for a 1.52 ppm C_2H_2 gas are measured at a rate of 0.5 Hz for a time range longer than 4 hours. The corresponding Allan-Werle plot shows the detection sensitivity of 7.8×10^{-10} cm^{-1} could be achieved at the integration time of 200 s. Finally, the linearity of the system has been validated by the measurement with different gas concentrations.

Optics EXPRESS

On the other hand, the advantage of the f-EOM of high bandwidth hasn't fully exploited in this work. This merits would be much more useful if uninterrupted locking of laser to one cavity longitudinal mode, realized by the method similar with Pound-Drever-Halling locking, is aimed [13,17]. According to our preliminary experiment, the locking bandwidth of 50 kHz could be achieved by using the f-EOM, which is much larger than that by a PZT, which often restricts the bandwidth in kHz range [17].

Funding. National Key Research and Development Program of China (2017YFA0304203); National Natural Science Foundation of China (61875107, 61905134, 61905136, 62175139); Scientific and Technological Innovation Programs of Higher Education Institutions in Shanxi (2019L0062).

Disclosures. The authors declare no conflicts of interest.

Data availability. Data underlying the results presented in this paper are not publicly available at this time but may be obtained from the authors upon reasonable request.

References

1. G. B. Rieker, J. B. Jeffries, and R. K. Hanson, "Calibration-free wavelength-modulation spectroscopy for measurements of gas temperature and concentration in harsh environments," Opt. Lett. **48**(29), 5546–5560 (2009).
2. J. Chen, A. Hangauer, R. Strzoda, and M. C. Amann, "Laser spectroscopic oxygen sensor using diffuse reflector based optical cell and advanced signal processing," Appl. Phys. B **100**(2), 417–425 (2010).
3. G. Gagliardi and H.-P. Loock, *Cavity-Enhanced Spectroscopy and Sensing*, (Springer, 2014).
4. G. D. Cole, W. Zhang, M. J. Martin, J. Ye, and M. Aspelmeyer, "Tenfold reduction of Brownian noise in high-reflectivity optical coatings," Nat. Photonics **7**(8), 644–650 (2013).
5. J. J. Scherer, J. B. Paul, A. Okeefe, and R. J. Saykally, "Cavity ringdown laser absorption spectroscopy: History, development, and application to pulsed molecular beams," Chem. Rev. **97**(1), 25–52 (1997).
6. J. B. Paul, C. P. Collier, R. J. Saykally, J. J. Scherer, and A. Okeefe, "Direct measurement of water cluster concentrations by infrared cavity ringdown laser absorption spectroscopy," J. Phys. Chem. A **101**(29), 5211–5214 (1997).
7. Y. Kitaoka, H. Sato, K. Mizuuchi, K. Yamamoto, and M. Kato, "Intensity noise of laser diodes with optical feedback," IEEE J. Quantum Electron. **32**(5), 822–828 (1996).
8. J. Morville, S. Kassi, M. Chenevier, and D. Romanini, "Fast, low-noise, mode-by-mode, cavity-enhanced absorption spectroscopy by diode-laser self-locking," Appl. Phys. B **80**(8), 1027–1038 (2005).
9. J. Morville, D. Romanini, A. A. Kachanov, and M. Chenevier, "Two schemes for trace detection using cavity ringdown spectroscopy," Appl. Phys. B **78**(3-4), 465–476 (2004).
10. A. G. V. Bergin, G. Hancock, G. A. D. Ritchie, and D. Weidmann, "Linear cavity optical-feedback cavity-enhanced absorption spectroscopy with a quantum cascade laser," Opt. Lett. **38**(14), 2475–2477 (2013).
11. K. M. Manfred, L. Ciaffoni, and G. A. D. Ritchie, "Optical-feedback cavity-enhanced absorption spectroscopy in a linear cavity: model and experiments," Appl. Phys. B **120**(2), 329–339 (2015).
12. R. Salter, J. Chu, and M. Hippler, "Cavity-enhanced Raman spectroscopy with optical feedback cw diode lasers for gas phase analysis and spectroscopy," Analyst **137**(20), 4669–4676 (2012).
13. J. F. Tian, G. Zhao, A. J. Fleisher, W. G. Ma, and S. T. Jia, "Optical feedback linear cavity enhanced absorption spectroscopy," Opt. Express **29**(17), 26831–26840 (2021).
14. Z. F. Luo, Z. Q. Tan, and X. W. Long, "Application of Near-Infrared Optical Feedback Cavity Enhanced Absorption Spectroscopy (OF-CEAS) to the Detection of Ammonia in Exhaled Human Breath," Sensors **19**(17), 3686 (2019).
15. M. Hippler, "Cavity-Enhanced Raman Spectroscopy of Natural Gas with Optical Feedback cw-Diode Lasers," Anal. Chem. **87**(15), 7803–7809 (2015).
16. A. Pelletier, P. Micheau, and A. Berry, "Implementation of a self-sensing piezoelectric actuator for vibro-acoustic active control," in *Conference on Sensors and Smart Structures Technologies for Civil, Mechanical, and Aerospace Systems*, J. P. Lynch, K.-W. Wang, and H. Sohn, eds. (Proceedings of SPIE, 2014), pp. 906149.
17. G. Zhao, J. Tian, J. T. Hodges, and A. J. Fleisher, "Frequency stabilization of a quantum cascade laser by resonant feedback from a linear two-mirror cavity," Opt. Lett. **46**(13), 3057–3060 (2021).
18. P. Laurent, A. Clairon, and C. Breant, "Frequency noise analysis of optically self-locked diode lasers," IEEE J. Quantum Electron. **25**(6), 1131–1142 (1989).
19. N. Schunk and K. Petermann, "Numerical analysis of the feedback regimes for a single-mode semiconductor laser with external feedback," IEEE J. Quantum Electron. **24**(7), 1242–1247 (1988).
20. P. Kluczynski, M. Jahjah, L. Nahle, O. Axner, S. Belahsene, M. Fischer, J. Koeth, Y. Rouillard, J. Westberg, A. Vicet, and S. Lundqvist, "Detection of acetylene impurities in ethylene and polyethylene manufacturing processes using tunable diode laser spectroscopy in the 3 μm range," Appl. Phys. B **105**(2), 427–434 (2011).
21. S. Wagner, M. Klein, T. Kathrotia, U. Riedel, T. Kissel, A. Dreizler, and V. Ebert, "In situ TDLAS measurement of absolute acetylene concentration profiles in a non-premixed laminar counter-flow flame," Appl. Phys. B **107**(3), 585–589 (2012).

Optics EXPRESS

22. Z. R. Quine and K. L. McNesby, "Acetylene measurement in flames by chirp-based quantum cascade laser spectrometry," Appl. Opt. **48**(16), 3075–3083 (2009).
23. E. A. Hardin, D. Stoller, J. Lawley, E. J. Howden, M. Hieda, J. Pawelczyk, S. Jarvis, K. Prisk, S. Sarma, and B. D. Levine, "Noninvasive Assessment of Cardiac Output: Accuracy and Precision of the Closed-Circuit Acetylene Rebreathing Technique for Cardiac Output Measurement," J. Am. Heart Assoc. **9**(17), 230–237 (2020).
24. M. Metsala, F. M. Schmidt, M. Skytta, O. Vaittinen, and L. Halonen, "Acetylene in breath: background levels and real-time elimination kinetics after smoking," J. Breath Res. **4**(4), 046003 (2010).
25. G. Zhao, T. Hausmaninger, F. M. Schmidt, W. Ma, and O. Axner, "High-resolution trace gas detection by sub-Doppler noise-immune cavity-enhanced optical heterodyne molecular spectrometry: application to detection of acetylene in human breath," Opt. Express **27**(13), 17940–17953 (2019).
26. P. C. D. Hobbs, "Ultrasensitive laser measurements without tears," Appl. Opt. **36**(4), 903–920 (1997).
27. I. E. Gordon, L. S. Rothman, C. Hill, R. V. Kochanov, Y. Tan, P. F. Bernath, M. Birk, V. Boudon, A. Campargue, K. V. Chance, B. J. Drouin, J. M. Flaud, R. R. Gamache, J. T. Hodges, D. Jacquemart, V. I. Perevalov, A. Perrin, K. P. Shine, M. A. H. Smith, J. Tennyson, G. C. Toon, H. Tran, V. G. Tyuterev, A. Barbe, A. G. Csaszar, V. M. Devi, T. Furtenbacher, J. J. Harrison, J. M. Hartmann, A. Jolly, T. J. Johnson, T. Karman, I. Kleiner, A. A. Kyuberis, J. Loos, O. M. Lyulin, S. T. Massie, S. N. Mikhailenko, N. Moazzen-Ahmadi, H. S. P. Muller, O. V. Naumenko, A. V. Nikitin, O. L. Polyansky, M. Rey, M. Rotger, S. W. Sharpe, K. Sung, E. Starikova, S. A. Tashkun, J. Vander Auwera, G. Wagner, J. Wilzewski, P. Wcislo, S. Yu, and E. J. Zak, "The HITRAN2016 molecular spectroscopic database," J. Quant. Spectrosc. Ra. **203**, 3–69 (2017).
28. D. W. Allan, "Should the classical variance be used as a basic measure in standards metrology?" IEEE Trans. Instrum. Meas. **IM-36**(2), 646–654 (1987).

210.0.158.151 {ts '2022-02-11 19:44:39'}